Materials Science and Engineering C 76 (2017) 856–864

Contents lists available at ScienceDirect

Materials Science and Engineering C

journal homepage: www.elsevier.com/locate/msec

Facile synthesis of fluorescence carbon dots from sweet potato for Fe^{3+} sensing and cell imaging

Jie Shen [a], Shaoming Shang [a,*], Xiuying Chen [a], Dan Wang [b], Yan Cai [c]

[a] School of Chemical and Material Engineering, Jiangnan University, Wuxi 214122, China
[b] State Key Laboratory of Organic-Inorganic Composites, Beijing University of Chemical Technology, Beijing 100029, China
[c] School of Chemistry and Chemical Engineering, Nantong University, Nantong 226019, China

ARTICLE INFO

Article history:
Received 27 October 2016
Received in revised form 7 February 2017
Accepted 21 March 2017
Available online 22 March 2017

Keywords:
Carbon dots
Fluorescence
Biomass
Biological imaging
Fe^{3+} detection

ABSTRACT

In this study, a facile synthesis of fluorescence carbon dots (CDs) from sweet potato was performed through hydrothermal treatment. The obtained CDs with quantum yield of 8.64% have good dispersibility due to the soluble functional groups on their surfaces. The characterization of CDs was carried out and their possible formation mechanism was also discussed. In addition, the cytotoxicity results showed that the CDs exhibit non toxicity within 100 μg/mL. At this concentration, the CDs were applied in cell imaging, indicating that they are promising fluorescent probes for biological imaging. In addition, the fluorescence of CDs was quenched by Fe^{3+} with a linear concentration of 1 to 100 μM, associated with the limit of detection of 0.32 μM. Subsequently, the CDs were successfully applied for Fe^{3+} probing in living cells.

1. Introduction

Carbon dots (CDs) are a kind of newly emerging nano-materials with the size less than 10 nm. Since they were discovered accidently during the separation and purification of single-walled carbon nanotubes [1], CDs have been proved to have many excellent properties. One of the important properties is their valuable photoluminescence. Compared with the traditional fluorescent dyes, CDs exhibit more superior fluorescence including photostability, resistance to photobleaching and non-blinking. Besides, CDs have other fascinating characteristics such as water-solubility, low toxicity, high chemical stability, easy functionalization [2,3] and satisfying biocompatibility [4–6]. Thus, CDs are explored to be applied in bioimaging [7–9], photocatalysis [10], sensing [11–14] and light-emitting devices [15–17].

Due to the excellent properties and extensive application of CDs, much research has focused on the synthesis of CDs [18–28]. Recently, many efforts have been devoted to the hydrothermal synthesis using bio-resource as precursor [29–33]. For hydrothermal synthesis, it has a great many advantages such as simple preparation, easy control of reaction, and low energy-consumption. Especially, hydrothermal synthesis can make the CDs self-passivated without any post-treatment. Employing bio-resource as precursor is not only due to its abundance, low cost and non toxicity but also because of its Green Chem nature. It is well known that bio-resource has plenty of carbohydrates such as sugar, starch, and polysaccharides. Besides C element, carbohydrates are composed of O, and H elements which facilitate the synthesis of CDs with functional groups (e.g. OH, COOH) on their surface. These functional groups are benefit to improve water-solubility and fluorescence of CDs. Much research has successfully prepared CDs by hydrothermal synthesis using carbohydrates from bio-resource as precursors. Liu [34] and Basu [35] employed starch from different biomass as raw material to synthesize CDs for bioimaging and fluoride ion detection, respectively. Zhou et al. [36] developed a facile one-step approach towards amphibious CDs based on the hydrothermal carbonization of polysaccharide from peach gum. The obtained CDs exhibit excellent solubility and strong photoluminescence both in water and organic solvents. Since bio-resource is abundant in carbohydrates, many researchers directly use bio-resource as precursor instead of the corresponding carbohydrates. Mehta et al. [37] employed apple juice to fabricate CDs for imaging of mycobacterium and fungal cells. Meanwhile, this research group also developed a hydrothermal synthesis of multicolor emission CDs from potato for HeLa cells imaging. Prasannan and Imae [30] described the hydrothermal carbonization of orange waste peels to prepare CDs, which has great potential in catalytic system. Although using bio-resource for synthesis of CDs has been confirmed to be effective strategy, it is still a challenge to explore new bio-resource to prepare the CDs with satisfying properties.

* Corresponding author.
E-mail address: smshangpaper@163.com (S. Shang).

http://dx.doi.org/10.1016/j.msec.2017.03.178
0928-4931/

Recently, the CDs are widely employed as fluorescent probes in sensing. With the extensive development of CDs prepared from bio-resource, the corresponding applications have been explored. For instance, the CDs respectively prepared from eggshell membrane [38], prawn shells [39] and bamboo leaves [40] have the ability to detect Cu^{2+}. Meanwhile, using pomelo peel [41], potato and cucumber [42] as carbon source can produce the CDs for Hg^{2+} assay. It is reported that CDs originated from banana peels [43], potatoes [29] can be used for Fe^{3+} sensing. These capacities for Cu^{2+}, Hg^{2+} and Fe^{3+} sensing are respectively due to amino groups, carboxyl groups and hydroxyl groups on the surface of CDs [44]. Besides ions assaying, the CDs from bio-resource for detecting small molecules including methylene blue [45], tetracycline [46] and glucose [47] are in literatures. In addition, Hsu et al. [48] found that the CDs synthesized from green tea presented excellent anticancer features. It is suggested that the specific applications of these CDs are attributed to the difference of bio-resource, resulting in the various chemical structures. Although the CDs with new sensing abilities has been reported continually, the efforts are still paid on to shed light on the detailed sensing mechanism.

Sweet potato is a worldwide agriculture product with high yield. Thus, it provides enough raw material to fabricate CDs in large scale. Previously, Zheng et al. [49] has employed sweet potato to prepare CDs by pyrolysis carbonization at 800 °C. Herein, the sweet potato was carbonized by hydrothermal treatment which is more convenient and eco-friendly (Fig. 1). The microstructure and chemical composition of the CDs were analyzed. Furthermore, the CDs were applied in cell imaging, showing that the CDs are promising multicolor fluorescent probes in biological field. The selectivity and sensitivity of the CDs for Fe^{3+} assay was performed and this detection was successfully applied in imaging of living cells.

2. Experimental section

2.1. Materials

Fresh sweet potato was purchased from local market. 3-(4,5-Dimethylthiazol-2-yl)-2,5-diphenyltetrazolium bromide (MTT) and quinine sulfate were purchased from Sigma, USA. Dulbecco's modified eagle's medium (DMEM) was obtained from Gibco, USA. Fetal bovine serum was purchased from Sijiqing, China. All other chemical reagents were purchased from Sinopharm Chemical Reagent Co., Ltd.

2.2. Preparation of CDs

The fluorescent CDs were synthesized by hydrothermal treatment using the extraction from sweet potato as carbon source. Briefly, 100 g fresh sweet potato was cut into small pieces and was added 350 mL deionized water. The mixture was blended by high speed tissue blender to crush the cells of sweet potato. Subsequently, the mixture was heated at 80 °C for 3 h under magnetic stirring. Then the mixture was centrifuged at 8000 rpm for 20 min to discard precipitation. The obtain supernatant was transferred into an autoclave and heated constantly at 180 °C for 18 h. After heating, the autoclave was cooled down to room temperature naturally. The obtained dark solution was centrifuged at 10,000 rpm for 15 min, then filtered through a 0.22 μm microporous membrane to remove large particles. The CDs were dialysed for 48 h against deionized water.

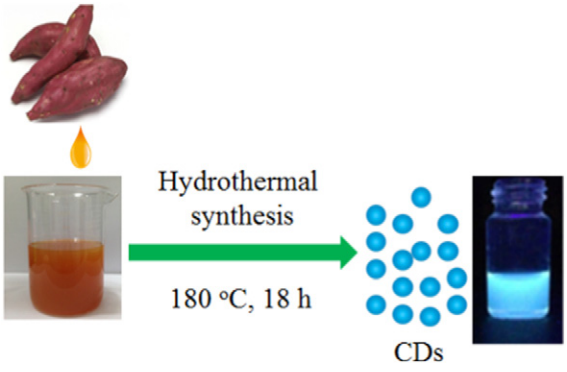

Fig. 1. Illustration of the formation of CDs from sweet potato.

2.3. Quantum yield calculation

The quantum yield (QY) of CDs was determined by comparing the integrated photoluminescence intensities (excited at 360 nm) and the absorbance values (at 360 nm) of CDs, using quinine sulfate as a reference. The QY was calculated as follows:

$$QY_S = QY_{ST}(I_S/I_{ST})(A_{ST}/A_S)(\eta_S/\eta_{ST})^2$$

where I refers to the integrated photoluminescence intensities, A represents the absorbance value, η denotes the refractive index of the solvent (both are 1.33). The subscript "S" and "ST" refer to CDs and quinine sulfate, respectively. The quinine sulfate was in 0.1 M H_2SO_4 with QY_{ST} of 54%. In order to minimize the reabsorption effect, the absorbance value was recorded below 0.05.

2.4. Characterization methods

UV–Vis absorption spectra were recorded by a TU–1991 UV–Vis spectrophotometer. Photoluminescence (PL) measurements were performed on a Shimadzu RF–5301 spectrofluorimeter. Fourier transform infrared spectroscopy (FTIR) was measured by a Nicolet 6700 FTIR spectrophotometer. The morphology and microstructure of CDs were characterized using JEM–2100 transmission electron microscope (TEM) with an accelerating voltage of 200 kV. X-ray diffraction (XRD) pattern was obtained by a Bruker D2-phaser diffractometer. X-ray photoelectron spectroscopy (XPS) measurements were carried out on a VG ESCALAB 220i-XL surface analysis system. The cell viability was detected on a Multiskan MK3 auto enzymelabeled meter. Cell imagings were performed on a Carl Zeiss 510 LSM laser scanning confocal microscope.

2.5. Cell culture

The human epithelial carcinoma (HeLa) and human hepatocarcinoma cells (HepG2) were obtained from Shanghai Institute of Biochemistry and Cell Biology, Chinese Academy of Science. The cells were cultured in DMEM medium supplemented with 10% fetal bovine serum, 100 U/mL penicillin, and 100 mg/mL streptomycin in a humidified 5% CO_2 atmosphere at 37 °C.

2.6. Cell viability assay

The cell viability assay was performed by MTT method. Briefly, cells were adjusted to 7×10^4/mL with DMEM complete medium. 100 μL of cells were seeded into 96-well plates and cultured for 24 h at 37 °C in 5% CO_2. The supernatant was removed and the cells were treated with different concentration of CDs (150 μL/well) for 24 h. The controls were treated with medium only. Then 15 μL of 5 mg/mL MTT was added into each well. After 4 h incubation, the medium was removed and 150 μL DMSO was added to dissolve the formazan crystals. The absorbance was measured at 490 nm on auto enzymelabeled meter. The cell viability was expressed as follows:

$$\text{cell viability}\ (\%) = \frac{\text{A490 of sample}}{\text{A490 of control}} \times 100\%$$

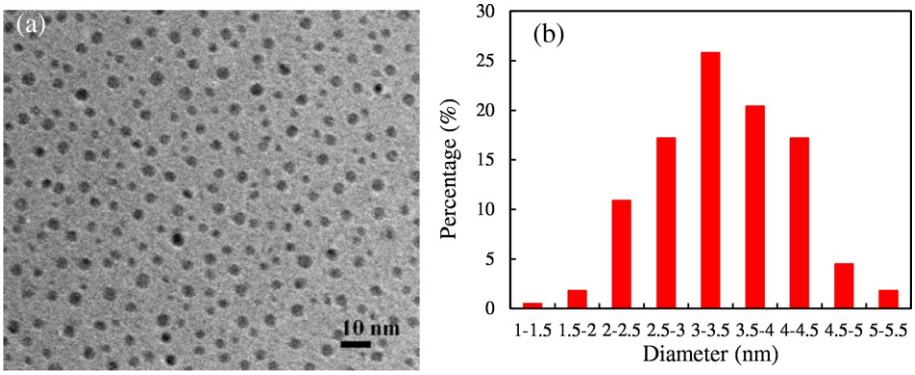

Fig. 2. (a) TEM image of CDs; (b) particle size distribution of CDs.

2.7. Cellular imaging

The cells were seeded in 6-well plates with a density of 1×10^4 per well. After incubation for 24 h, the cells were treated with 100 μg/mL CDs for 4 h. Then the cells were washed 3 times by phosphate buffered saline (PBS) to remove medium and the free CDs. As for Fe^{3+} detection, 200 μM of Fe^{3+} was added into the CDs treated cells for another 2 h. Then, the cells were washed again by PBS for 3 times. Finally, the cells were imaged by confocal fluorescence microscopy.

2.8. Fluorescence sensing of Fe^{3+}

In a typical assay, 35 mg of CDs was dissolved in 500 mL water. 40 μL of a certain concentration of Fe^{3+} was added into 5 mL CDs solution. The final concentration of Fe^{3+} was in the range of 0–500 μM. The fluorescence spectra were recorded at an excitation wavelength of 360 nm. To evaluate the selectivity towards Fe^{3+}, different metal ions with the concentration of 100 μM were added into CDs solution in a same way. All the measurements were conducted in triples.

3. Result and discussion

3.1. Synthesis of CDs

The CDs were prepared by hydrothermal synthesis from sweet potato which contains carbohydrates. It is known that carbohydrates act as various biological roles and exist considerably in cells. In order to obtain the carbohydrates as more as possible, it is effective to crush the cells of sweet potato, making the cells released carbohydrates. Thus, the sweet potato mixed with water was firstly blended by high speed tissue blender and then heated at 80 °C for 3.5 h to break the cell wall. Consequently, numerous carbohydrates were released and easily solved in water. These steps above are similar to those that preparing crude polysaccharides from sweet potato with high yield [50], confirming that it provides enough carbon-based precursor.

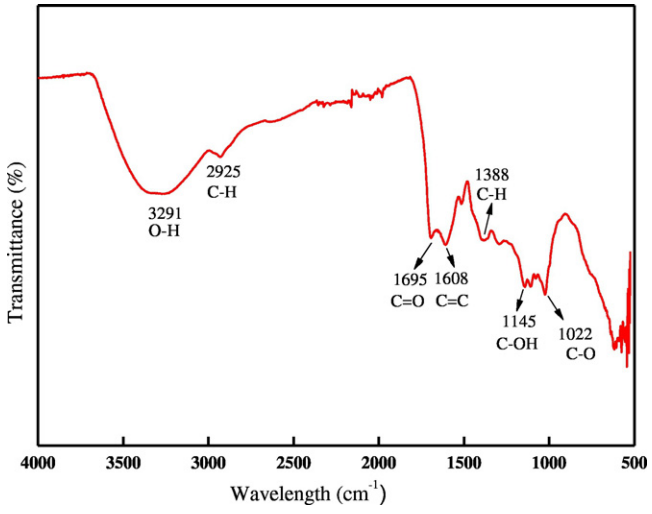

Fig. 3. The FTIR spectrum of CDs.

Besides carbohydrates, the cells from bio-resource also contain other biological molecules like proteins. Recently, it is proposed that doping with N element on CDs can effectively improve and tune their fluorescence properties. Many researchers have selected proteins as N source and successfully synthesized N-doped CDs [51, 52]. In this study, we employed sweet potato as precursor, expecting to prepare the CDs that contain both C and N elements. However, the following results showed that no N element takes part in the synthesis. Since the sweet potato juice was heated at higher temperature for several hours, probably resulting in the denaturation of proteins. Subsequently, these proteins were precipitation and removed together with pulp. In addition, other bio-resource like apple [37], *Saccharum officinarum* [53] and potato [29] was treated without heating process, but still no or little amount of N element was detected by analysis. Obviously, it is implied that no or just less proteins participate in the reaction. It may be explained that there are no appropriate functional groups of carbohydrates for proteins to make their N element connected on their surface. It is suggested that to dope with N element on CDs prepared from carbohydrates, choosing small molecules as passivated agent is an effective approach [54].

Up to now, a lot of CDs with different synthetic methods and raw materials have been reported. Previously, the CDs were obtained by cutting mass carbon based materials which is called as “top-down methods”. However, these methods commonly need expensive and complicated equipment, tedious processes and hash reaction conditions. Furthermore, the QY and biocompatibility of the resulting CDs are not satisfying. Meanwhile, “bottom-up approaches” for CDs synthesis have been reported in literatures, such as hydrothermal treatment and microwave synthesis [55]. It is found that hydrothermal treatment which was employed in this study is more efficient than microwave synthesis, especially using bio-resource as carbon source. Hydrothermal treatment is an easily controlled conventional heating method. It can provide continuous heating energy even up to high temperature that benefits the carbonation of bio-resource. As for microwave synthesis, the heating effect is originated from electromagnetic energy. In addition, it is difficult to control irradiation power and absorption properties of precursors [56], resulting in poor reproducibility, as well as low quality of CDs from bio-resource. Besides synthetic methods, the raw materials and reaction conditions also play an important role in carbonation and surface passivation during the formation of CDs. Subsequently, it is contributed to the different CDs with various chemical structure and properties including optical properties.

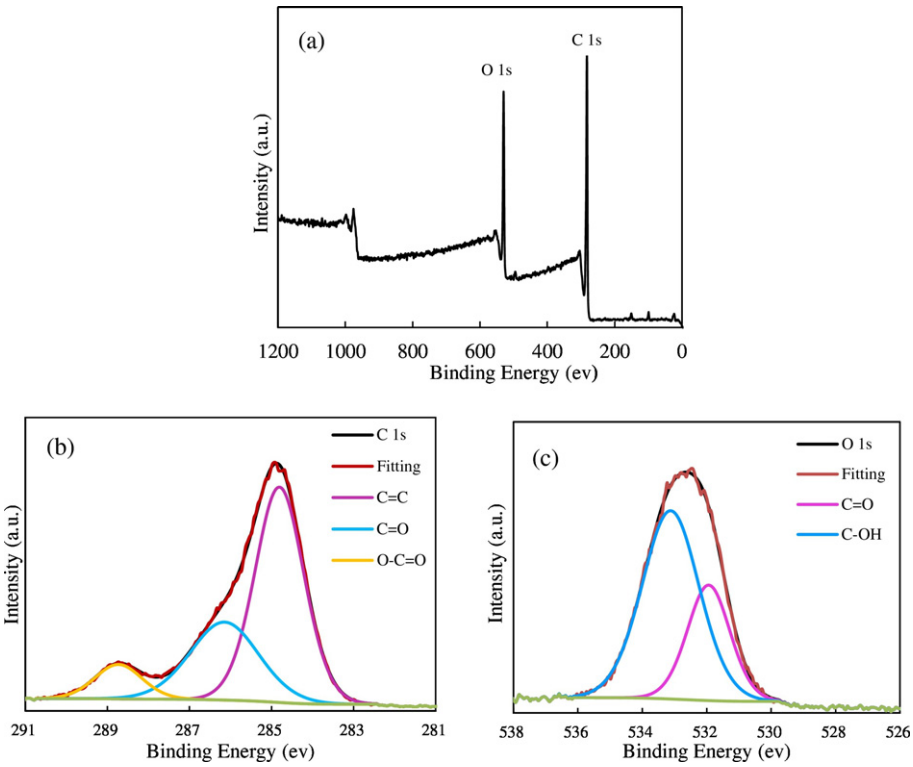

Fig. 4. (a) XPS survey spectrum, (b) C 1s and (c) O 1s high resolution XPS spectra of CDs.

Although the mechanism of the formation of CDs from carbohydrates has been extensively investigated, the detailed pathway of synthesis is still unknown. It may be explained that the carbohydrates from sweet potato is initially hydrolyzed into monosaccharides such as glucose. Sun et al. [57] suggested that the growth of carbon spheres prepared from glucose conforms the LaMer model [58], and the temperature is higher than 140 °C. In our experiments, the reaction was performed at 180 °C which is benefit to form the carbon spheres. Subsequently, the monosaccharides are dehydrated into furfural intermediates. These intermediates further turn into aromatic compounds and oligosaccharides due to the polymerization step. As the reaction solution reached a critical super-saturation, a single burst of nucleation formed. This step is ascribed to the dehydration of linear or branchlike oligosaccharides, or other macromolecules. Then the nuclei grows uniformly and isotropically during the solute diffused towards the particle surface. At last, the grown carbon substances are oxidized to improve their properties such as water solubility. However, in the processes of hydrolysis, dehydration and polymerization, it is still a great challenge to characterize the intermediates in every step, consequently leading to the undefined formation of CDs from carbohydrates.

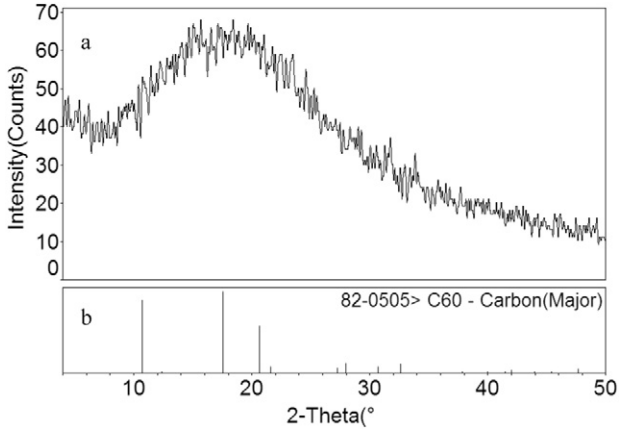

Fig. 5. XRD pattern of CDs (a) and the standard spectrum of C60 (b).

3.2. Characterization of CDs

The morphology and size distribution of CDs were characterized by TEM. As shown in Fig. 2(a), the CDs are spherical in shape and well separated from each other. Fig. 2(b) displays the size distribution of the CDs which are mainly in the range of 2.5–5.5 nm. The average diameter of the CDs is 3.39 nm. To identify the chemical structure of CDs, FTIR spectroscopy was performed. As it can be seen in Fig. 3, a broad band around 3291 cm^{-1} is ascribed to the stretching vibrations of —OH. A peak at 2925 cm^{-1} is assigned to the stretching vibrations of C—H. A peak at 1695 cm^{-1} indicates the existence of C═O. A peak at 1608 cm^{-1} is the result of the stretching vibrations of C═C. A peak centered at 1388 cm^{-1} is corresponding to the bending vibrations of C—H. A peak at 1145 cm^{-1} is assigned to the stretching vibrations of C—OH. A peak at 1022 cm^{-1} is originated from the stretching vibrations of C—O. XPS provides the information about the elemental composition and chemical bond of CDs. The XPS survey spectrum in Fig. 4(a) implies that the CDs contain two kinds of elements: C and O elements. The atomic ratio of C to O is 78.6/19.9, implying that the CDs are mainly composed of C element. Fig. 4(b) and (c) shows the high-resolution XPS spectrum of C1s and O1s, respectively. The spectrum of C1s of which binding energy is 284.98 ev is divided into three peaks. These peaks centered at 284.78, 286.28 and 288.83 ev are respectively corresponding to C═C, C═O, and O—C═O bonds. The O1s occurs at the peak of 532.78 ev and its spectrum is fitted with two peaks centered at 533.03 and 531.78 ev. These peaks represents the C—OH and C═O bonds. It is obvious that the analysis of XPS spectrum is in good agreement with that of FTIR spectrum, confirming that the CDs contain OH and COOH groups. The presence of the two functional groups above improves the water-solubility of CDs. The XRD pattern in Fig. 5(a) presents a broad peak indicating that the CDs have the amorphous nature. In addition, the small sizes of CDs results in a broad diffraction peak width. Compared with the standard XRD pattern (Fig. 5(a)), the conformation

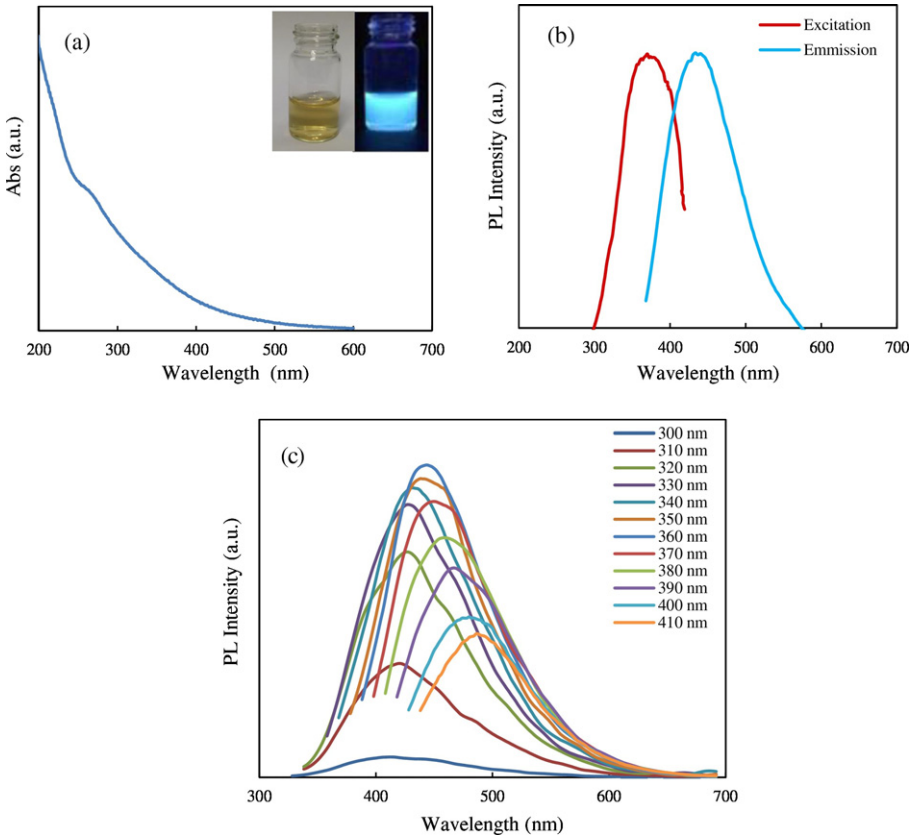

Fig. 6. (a) UV–Vis spectrum of CDs, inset picture shows the CDs under daylight (left) and UV light at 365 nm wavelength (right). (b) PL excitation and emission spectra, (c) PL emission spectra of the CDs different excitation wavelengths.

of CDs is mostly similar to that of fullerene (C60), implying that the CDs have non plane structure but own sp2 and sp3 carbon clusters.

3.3. Optical properties of CDs

The UV–Vis spectrum of CDs is shown in Fig. 6(a). The CDs have an optical absorption in UV region, with a tail extended to the visible region. The absorption peak at 266 nm is assigned to the π-π*transition of C═C. This is the characterization of the CDs prepared by the carbonization of carbon based materials [30]. As it can be seen in Fig. 6(b), the maximum emission peak of CDs is 442 nm as it is excited at 360 nm. Excitation-dependent PL behavior is typical and common in carbon fluorescent materials. This phenomenon is also observed in Fig. 6(c) that the PL emission peak of the CDs is shifted from 406 to 486 nm with the excitation wavelength varied from 300 nm to 410 nm. The reason why the PL emission peak is red-shifted as the corresponding excitation wavelength increased is not very clear. The plausible explanations are ascribed to the different particle size and the distribution of various emissive sites on the CDs surface. Consequently, it results in the fact that the particles with smaller sizes get excited at lower wavelengths while the larger size of particles are excited at higher wavelengths [37]. In this study, the QY of CDs is calculated at 8.64% using quinine sulfate (0.1 M H_2SO_4 as solvent; QY = 54%) as a reference. As for the mechanism of photoluminescence, there exists two plausible theories. One of the theories is defect state emission, the other is intrinsic emission [59]. In addition, it is suggested that the oxidation of CDs affect their PL properties. The CDs with higher oxidation degree own more surface states, leading to the PL emission with varied energies at different excitations [60]. Thus, doping with O element is an efficient way to control PL emission and increase QY.

Employing bio-resource as precursor provides a new pathway to prepare CDs with idea biocompatibility. However, the resulting CDs are

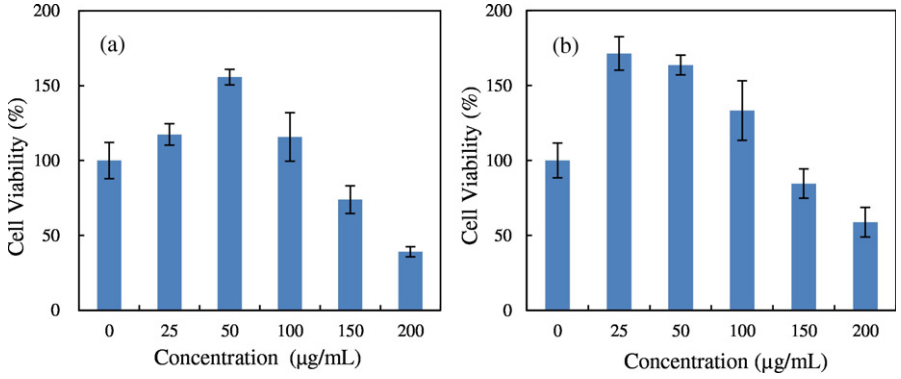

Fig. 7. The cell viabilities of HeLa (a) and HepG2 (b) cells.

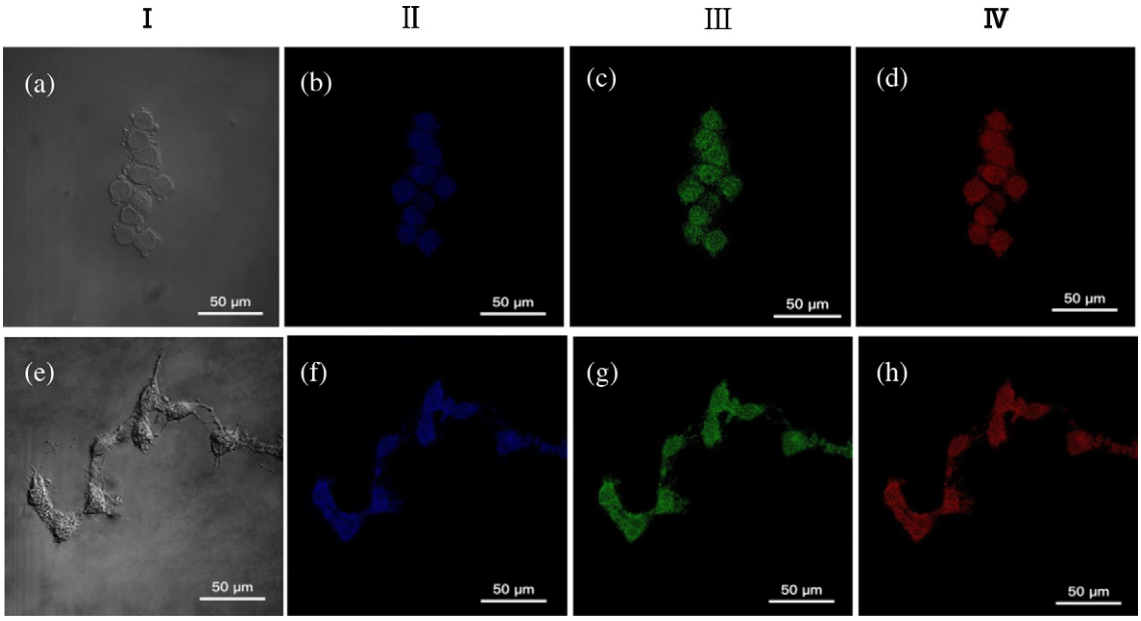

Fig. 8. Laser scanning confocal microscopy images of HeLa cells (a–d) and HepG2 cells (e–h). I, bright field; II, excited at 330–388 nm; III, excited at 450–480 nm; IV, excited at 510–550 nm. (For interpretation of the references to color in this figure, the reader is referred to the web version of this article.)

confronted with lower QY than those synthesized from compounds in most cases [42,53,61]. As discussed above, bio-resource is a mixture that contains various kinds of carbohydrates, leading to different carbonation in a certain reaction condition. Furthermore, the QY of CDs synthesized from bio-resource depends on the content of effective components which produce high QY. Lu et al. [62] suggested that they synthesized CDs from sweet potato by hydrothermal treatment had the QY of 2.8%, lower than ours. This difference may be ascribed to the pretreatment of the sweet potato. In this study, the sweet potato experienced the cell-wall crushed treatment, releasing more carbohydrates that may produce the CDs with high QY. In addition, the sweet potato juice was filtered to discard large particles, making the insoluble components dispersed well in water. On the contrary, Lu et al. [62] directly added sweet potato into water, probably resulting in the inhomogeneous carbonation and subsequently decrease the QY. Nowadays, with the deep exploration of bio-resource to synthesize CDs, the CDs with high QY have been described continuously. It is obvious that these CDs have been doped with hetero-atoms such as N and S elements [63–65]. The introduction of these

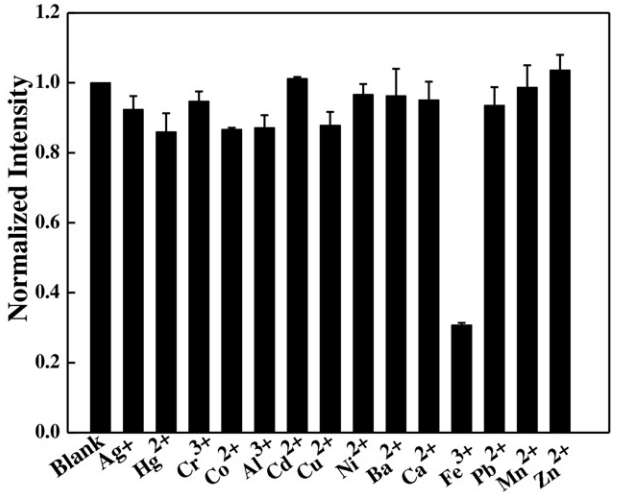

Fig. 9. Fluorescence responds of CDs towards different metal ions (100 μM).

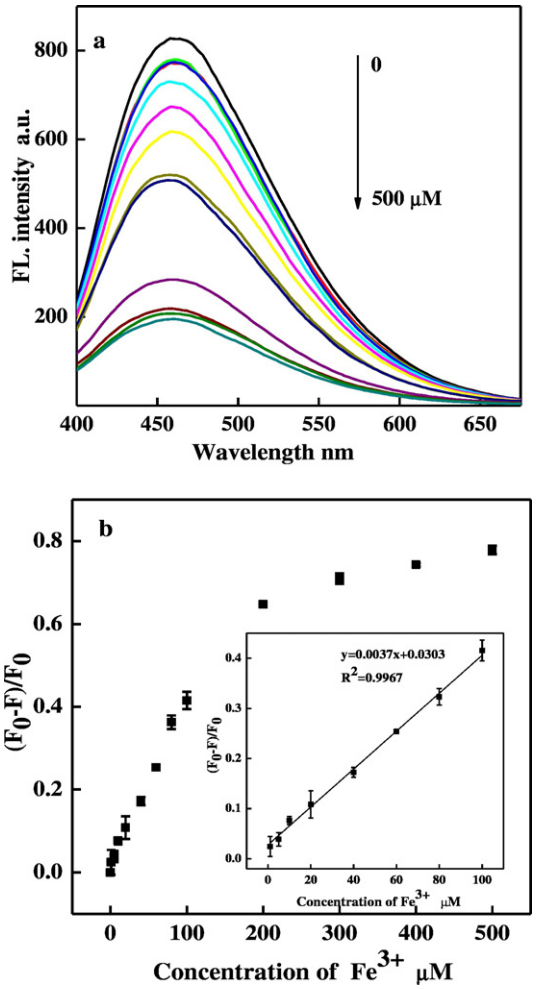

Fig. 10. (a) The fluorescence response of CDs towards addition of different concentration of Fe^{3+}; (b) The relationship between $(F_0\text{-}F)/F_0$ and concentration of Fe^{3+}, inset: a linear relationship with the concentration of Fe^{3+}; ranged from 1 to 100 μM.

elements on the surface of CDs can generate additional energy lever between π and π* of carbons, thus improving QY [66].

3.4. Cellular toxicity

The toxicity of CDs is always received great attention in biological application. Fig. 7 demonstrates the cell viabilities of HeLa and HepG2 cells which were treated with CDs for 24 h. As it can be seen in Fig. 7(a) the CDs promoted HeLa cells growth as the concentration of CDs increased to 100 μg/mL. The maximum cell viability of HeLa cells was 156% when the concentration of CDs was up to 50 μg/mL. However, the viability of HeLa cells decreased with the concentration of CDs continuously increasing. As for HepG2 cells (Fig. 7(b)), the relationship between concentration of CDs and cell viability is quite similar to that for HeLa cells. The viability of HepG2 cells initially exceeded 100% with the concentration of CDs from 0 to 100 μg/mL. Especially, the cell viability of HepG2 cells was as high as 171% at the concentration of CDs of 25 μg/mL. As the concentration of CDs increased up to 150 μg/mL, the viability of HepG2 cells began to decrease. In a word, the CDs improved cell viabilities of both HeLa and HepG2 cells within the concentration of 100 μg/mL, showing that the CDs has no toxicity. As the concentration increased, the CDs gradually exhibited low toxicity and finally toxicity to the two cells. Thus, it is worth noting that applying CDs in biological field should be taken their safe concentration into account.

In the previous paragraph, it is found that the conformation of CDs is mostly like that of fullerene. It has been reported that the fullerene suppressed HepG2 cells growth at a very low concentration [67]. Therefore, it may be speculated that the fullerene-like conformation lead to the CDs have cytotoxic property.

3.5. Cell imaging

Fig. 8 presents the confocal imaging of HeLa and HepG2 cells which were treated with CDs at the concentration of 100 μg/mL for 4 h. It is

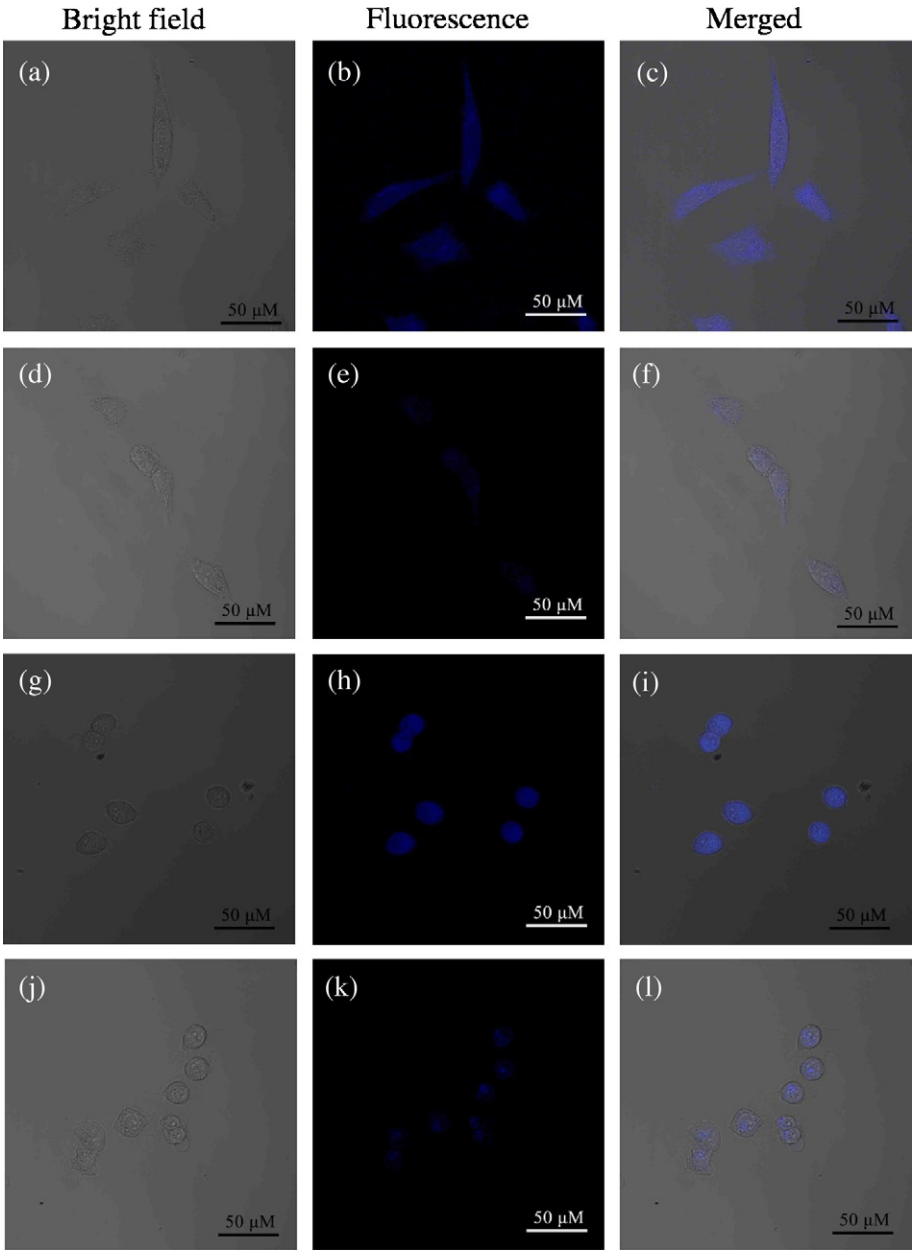

Fig. 11. Confocal images of Hela (a)–(f) and HepG2 (g)–(l). (a)–(c) and (g)–(i) are the cells incubated with CDs; (d)–(f) and (j)–(l) are the cells incubated with CDs and Fe^{3+}. The fluorescence images were obtained at 405 nm. (For interpretation of the references to color in this figure, the reader is referred to the web version of this article.)

shown that the CDs are successfully penetrated into the two cells because of the small sizes and hydrophilic functional groups on their surfaces. These cells emitted blue, green, and red fluorescence under ultraviolet (330–388 nm), blue (450–480 nm), and green (510–550 nm) light excitation, respectively. It is indicated that the CDs are biocompatible and suitable to be served as probes for cell imaging.

3.6. Selectivity and sensitivity for Fe^{3+} detection

Fig. 9 depicted the fluorescence responds of CDs in the presence of different metal ions. It is shown that Fe^{3+} had obvious fluorescent quenching effect while other ions had slight or no interference to fluorescence. Thus, it is indicating that the CDs have satisfying selectivity for Fe^{3+} assay. The mechanism of fluorescence quenching by Fe^{3+} is ascribed to the charge transfer and restrained exciton recombination [44]. It is proposed that the hydroxyl groups on the surface of CDs interacted with Fe^{3+}, leading to the electronic structure of CDs change. Moreover, Lu et al. [61] found that their synthesized CDs from sweet potato by hydrothermal treatment have high fluorescence selectivity towards Hg^{2+}. As they predicted that this fluorescence quenching is ascribed to strong affinity of Hg^{2+} to carboxylic group. In spite of using same carbon source and synthetic method, the obtained CDs have quite different property in ion sensing. Actually, the property of CDs is dependent on their chemical structure. As discussed above, the main species of functional group on the surface of CDs affect their specific recognition of foreign ions. It is no doubt that the two kinds of CDs prepared from sweet potato are different in chemical structure. The reason can be explained that the diverse pretreatment of sweet potato and reaction condition contribute to the difference of carbonation that affects the final structure.

The sensitivity of CDs for Fe^{3+} detection was estimated in this study. As Fig. 10(a) shown that, the fluorescent intensity of CDs decreased as the concentration of Fe^{3+} increased. Fig. 10(b) presents the relationship between fluorescent quenching ratio $(F_0\text{-}F)/F_0$ and Fe^{3+} concentration. As the concentration of Fe^{3+} was varied from 1 to 100 μM, a good linear was observed with the correlation coefficient square (R^2) of 0.9967. In addition, the limit of detection (LOD) was evaluated as 0.32 μM based on a signal-to-noise ratio of 3. According to the guideline limit of Fe^{3+} concentration (5.36 μM) proposed by World Health Organization (WHO), the LOD for Fe^{3+} detection in this study was much lower, showing that the CDs are promising in detecting trace amount of Fe^{3+}.

3.7. Fe^{3+} detection in living cells

The confocal images of Hela and HepG2 cells treated with CDs were performed for Fe^{3+} monitoring. As Fig. 11 indicated, both Hela and HepG2 cells only incubated with CDs (100 μg/mL) emitted strong blue fluorescence. However, as the Fe^{3+} (200 μM) penetrated into cells, the fluorescence faded dramatically. In total, it is indicated that the CDs have potential to monitoring Fe^{3+} in living cells.

4. Conclusion

In this study, a green and facile synthesis of CDs from sweet potato was developed. The CDs are spherical in shape with the average diameters of 3.39 nm. In addition, the characterization of CDs showed that they have oxygen containing groups on their surface which are benefit to the improvement of water solubility and fluorescence. The obtained CDs have good fluorescence with QY of 8.64%. Furthermore, the CDs were also applied in cell imaging at their non toxic concentration, indicating that they are promising multicolor fluorescent probes in biological imaging. In addition, it is shown that the CDs have satisfying selectivity and sensitivity for Fe^{3+} detection. The linear range of Fe^{3+} concentration was varied from 1 to 100 μM with a limit of detection as low as 0.32 μM. Furthermore, the application of Fe^{3+} detection was employed in living cells, showing that the CDs are promising as fluorescent sensors to detect Fe^{3+} in biological system.

Acknowledgements

This work was supported by the Fundamental Research Funds for the Central Universities (JUSRP11517), Youth Natural Science Foundation of Jiangsu Province (BK20150401), National Natural Science Foundation of China (51641201) and the Fundamental Research Funds for the Central Universities (BUCTRC201601).

References

[1] X.Y. Xu, R. Ray, Y.L. Gu, H.J. Ploehn, L. Gearheart, K. Raker, W.A. Scrivens, Electrophoretic analysis and purification of fluorescent single-walled carbon nanotube fragments, J. Am. Chem. Soc. 126 (2004) 12736–12737.
[2] K. Hola, A.B. Bourlinos, O. Kozak, K. Berka, K.M. Siskova, M. Havrdova, J. Tucek, K. Safarova, M. Otyepka, E.P. Giannelis, R. Zboril, Photoluminescence effects of graphitic core size and surface functional groups in carbon dots: COO-induced red-shift emission, Carbon 70 (2014) 279–286.
[3] S. Ruan, J. Wan, Y. Fu, K. Han, X. Li, J. Chen, Q. Zhang, S. Shen, Q. He, H. Gao, PEGylated fluorescent carbon nanoparticles for noninvasive heart imaging, Bioconjug. Chem. 25 (2014) 1061–1068.
[4] P. Zhang, Z. Xue, D. Luo, W. Yu, Z. Guo, T. Wang, Dual-peak electrogenerated chemiluminescence of carbon dots for iron ions detection, Anal. Chem. 86 (2014) 5620–5623.
[5] Z. Wang, Y. Qu, X. Gao, C. Mu, J. Bai, Q. Pu, Facile preparation of oligo(ethylene glycol)-capped fluorescent carbon dots from glutamic acid for plant cell imaging, Mater. Lett. 129 (2014) 122–125.
[6] F. Du, M. Zhang, X. Li, J. Li, X. Jiang, Z. Li, Y. Hua, G. Shao, J. Jin, Q. Shao, M. Zhou, A. Gong, Economical and green synthesis of bagasse-derived fluorescent carbon dots for biomedical applications, Nanotechnology 25 (2014) 1068–1072.
[7] H. Huang, Y.C. Lu, A.J. Wang, J.H. Liu, J.R. Chen, J.J. Feng, A facile, green, and solvent-free route to nitrogen-sulfur-codoped fluorescent carbon nanoparticles for cellular imaging, RSC Adv. 4 (2014) 11872–11875.
[8] Y. Song, S. Zhu, B. Yang, Bioimaging based on fluorescent carbon dots, RSC Adv. 4 (2014) 27184–27200.
[9] L. Wang, Y. Yin, A. Jain, H.S. Zhou, Aqueous phase synthesis of highly luminescent, nitrogen-doped carbon dots and their application as bioimaging agents, Langmuir 30 (2014) 14270–14275.
[10] S.L. Hu, Z.J. Wei, Q. Chang, A. Trinchi, J.L. Yang, Facile and green method towards coal-based fluorescent carbon dots with photocatalytic activity, Appl. Surf. Sci. 378 (2016) 402–407.
[11] M. Hu, Y. Yang, X. Gu, Y. Hu, J. Huang, C. Wang, One-pot synthesis of photoluminescent carbon nanodots by carbonization of cyclodextrin and their application in Ag^{+} detection, RSC Adv. 4 (2014) 62446–62452.
[12] G.H.G. Ahmed, R.B. Laino, J.A.G. Calzon, M.E.D. Garcia, Fluorescent carbon nanodots for sensitive and selective detection of tannic acid in wines, Talanta 132 (2015) 252–257.
[13] F. Yan, Y. Zou, M. Wang, X. Mu, N. Yang, L. Chen, Highly photoluminescent carbon dots-based fluorescent chemosensors for sensitive and selective detection of mercury ions and application of imaging in living cells, Sensors Actuators B Chem. 192 (2014) 488–495.
[14] Y. Wang, S. Wang, S. Ge, S. Wang, M. Yan, D. Zang, J. Yu, Facile and sensitive paper-based chemiluminescence DNA biosensor using carbon dots dotted nanoporous gold signal amplification label Anal, Methods 5 (2013) 1328–1336.
[15] F. Wang, Y.h. Chen, C.y. Liu, D.g. Ma, White light-emitting devices based on carbon dots' electroluminescence, Chem. Commun. 47 (2011) 3502–3504.
[16] L. Tang, R. Ji, X. Cao, J. Lin, H. Jiang, X. Li, K.S. Teng, C.M. Luk, S. Zeng, J. Hao, Deep ultraviolet photoluminescence of water-soluble self-passivated graphene quantum dots, ACS Nano 6 (2012) 5102–5110.
[17] L.H. Mao, W.Q. Tang, Z.Y. Deng, S.S. Liu, C.F. Wang, S. Chen, Facile access to white fluorescent carbon dots toward light-emitting devices, Ind. Eng. Chem. Res. 53 (2014) 6417–6425.
[18] A.Al. Hamaoy, E. Chikarakara, H. Jawad, K. Gupta, D. Kumar, M.S.R. Rao, S. Krishnamurthy, M. Morshed, E. Fox, D. Brougham, X. He, M. Vazquez, D. Brabazon, Liquid phase - pulsed laser ablation: a route to fabricate different carbon nanostructures, Appl. Surf. Sci. 302 (2014) 141–144.
[19] X. Li, H. Wang, Y. Shimizu, A. Pyatenko, K. Kawaguchi, N. Koshizaki, Preparation of carbon quantum dots with tunable photoluminescence by rapid laser passivation in ordinary organic solvents, Chem. Commun. 47 (2011) 932–934.
[20] K. Tulugan, H. Kim, W. Park, Y. Choi, W. Park, Aluminum-silicon and aluminum-silicon/carbon nanoparticles with core-shell structure synthesized by arc discharge method, J. Alloys Compd. 579 (2013) 529–532.
[21] C.I. Wang, W.C. Wu, A.P. Periasamy, H.T. Chang, Electrochemical synthesis of photoluminescent carbon nanodots from glycine for highly sensitive detection of hemoglobin, Green Chem. 16 (2014) 2509–2514.
[22] Z.A. Qiao, Y. Wang, Y. Gao, H. Li, T. Dai, Y. Liu, Q. Huo, Commercially activated carbon as the source for producing multicolor photoluminescent carbon dots by chemical oxidation, Chem. Commun. 46 (2010) 8812–8814.
[23] K. Guo, H. Qi, F. Wang, Y. Zhu, Fabrication of boron- and nitrogen-doped carbon nanoparticles by stress from pyrolysis of borazine-containing arylacetylene, RSC Adv. 4 (2014) 6330–6336.
[24] C.W. Lai, Y.H. Hsiao, Y.K. Peng, P.T. Chou, Facile synthesis of highly emissive carbon dots from pyrolysis of glycerol; gram scale production of carbon dots/mSiO(2) for cell imaging and drug release, J. Mater. Chem. 22 (2012) 14403–14409.

[25] C. Wang, Z. Xu, H. Cheng, H. Lin, M.G. Humphrey, C. Zhang, A hydrothermal route to water-stable luminescent carbon dots as nanosensors for pH and temperature, Carbon 82 (2015) 87–95.
[26] D. Kim, Y. Choi, E. Shin, Y.K. Jung, B.S. Kim, Sweet nanodot for biomedical imaging: carbon dot derived from xylitol, RSC Adv. 4 (2014) 23210–23213.
[27] E. Kianpour, S. Azizian, Optimization of one-step and one-substrate synthesis of carbon nanodots by microwave pyrolysis, RSC Adv. 4 (2014) 40907–40911.
[28] Y. Liu, N. Xiao, N. Gong, H. Wang, X. Shi, W. Gu, L. Ye, One-step microwave-assisted polyol synthesis of green luminescent carbon dots as optical nanoprobes, Carbon 68 (2014) 258–264.
[29] J. Xu, Y. Zhou, S. Liu, M. Dong, C. Huang, Low-cost synthesis of carbon nanodots from natural products used as a fluorescent probe for the detection of ferrum(III) ions in lake water, Anal. Methods 6 (2014) 2086–2090.
[30] A. Prasannan, T. Imae, One-pot synthesis of fluorescent carbon dots from orange waste peels, Ind. Eng. Chem. Res. 52 (2013) 15673–15678.
[31] V. Chaudhary, A.K. Bhowmick, Green synthesis of fluorescent carbon nanoparticles from lychee (*Litchi chinensis*) plant, Korean J. Chem. Eng. 32 (2015) 1707–1711.
[32] R. Atchudan, T. Edison, M.G. Sethuraman, Y.R. Lee, Efficient synthesis of highly fluorescent nitrogen-doped carbon dots for cell imaging using unripe fruit extract of *Prunus mume*, Appl. Surf. Sci. 384 (2016) 432–441.
[33] L. Shi, Y. Li, X. Li, X. Wen, G. Zhang, J. Yang, C. Dong, S. Shuang, Nano 7 (2015) 7394–7401.
[34] M. Liu, X. Zhang, B. Yang, Z. Li, F. Deng, Y. Yang, X. Zhang, Y. Wei, Carbohydr. Polym. 121 (2015) 49–55.
[35] A. Basu, A. Suryawanshi, B. Kumawat, A. Dandia, D. Guin, S.B. Ogale, Starch (Tapioca) to carbon dots: an efficient green approach to an on-off-on photoluminescence probe for fluoride ion sensing, Analyst 140 (2015) 1837–1841.
[36] L. Zhou, B. He, J. Huang, Fluorescent carbon dots: one-step green synthesis and application for light-emitting polymer nanocomposites, Chem. Commun. 49 (2013) 8078–8080.
[37] V.N. Mehta, S. Jha, H. Basu, R.K. Singhal, S.K. Kailasa, One-step hydrothermal approach to fabricate carbon dots from apple juice for imaging of mycobacterium and fungal cells, Sensors Actuators B Chem. 213 (2015) 434–443.
[38] Q. Wang, X. Liu, L. Zhang, Y. Lv, Microwave-assisted synthesis of carbon nanodots through an eggshell membrane and their fluorescent application, Analyst 137 (2012) 5392–5397.
[39] G. Gedda, C.Y. Lee, Y.C. Lin, H.F. Wu, Green synthesis of carbon dots from prawn shells for highly selective and sensitive detection of copper ions, Sensors Actuators B Chem. 224 (2016) 396–403.
[40] Y. Liu, Y. Zhao, Y. Zhang, One-step green synthesized fluorescent carbon nanodots from bamboo leaves for copper(II) ion detection, Sensors Actuators B Chem. 196 (2014) 647–652.
[41] W. Lu, X. Qin, S. Liu, G. Chang, Y. Zhang, Y. Luo, A.M. Asiri, A.O. Al-Youbi, X. Sun, Economical, green synthesis of fluorescent carbon nanoparticles and their use as probes for sensitive and selective detection of mercury(II) ions, Anal. Chem. 84 (2012) 5351–5357.
[42] C. Wang, D. Sun, K. Zhuo, H. Zhang, J. Wang, Simple and green synthesis of nitrogen-, sulfur-, and phosphorus-co-doped carbon dots with tunable luminescence properties and sensing application, RSC Adv. 4 (2014) 54060–54065.
[43] R. Vikneswaran, S. Ramesh, R. Yahya, Green synthesized carbon nanodots as a fluorescent probe for selective and sensitive detection of iron(III) ions, Mater. Lett. 136 (2014) 179–182.
[44] Y. Guo, L. Zhang, S. Zhang, Y. Yang, X. Chen, M. Zhang, Fluorescent carbon nanoparticles for the fluorescent detection of metal ions, Biosens. Bioelectron. 63 (2015) 61–71.
[45] M. Xue, M. Zou, J. Zhao, Z. Zhan, S. Zhao, Green preparation of fluorescent carbon dots from lychee seeds and their application for the selective detection of methylene blue and imaging in living cells, J. Mater. Chem. B 3 (2015) 6783–6789.
[46] Y. Feng, D. Zhong, H. Miao, X. Yang, Carbon dots derived from rose flowers for tetracycline sensing, Talanta 140 (2015) 128–133.
[47] D. Wu, X. Deng, X. Huang, K. Wang, Q. Liu, Low-cost preparation of photoluminescent carbon nanodots and application as peroxidase mimetics in colorimetric detection of H_2O_2 and glucose, J. Nanosci. Nanotechnol. 13 (2013) 6611–6616.
[48] P.C. Hsu, P.C. Chen, C.M. Ou, H.Y. Chang, H.T. Chang, Extremely high inhibition activity of photoluminescent carbon nanodots toward cancer cells, J. Mater. Chem. B 1 (2013) 1774–1781.
[49] P. Zheng, T. Liu, J. Zhang, L. Zhang, Y. Liu, J. Huang, S. Guo, Sweet potato-derived carbon nanoparticles as anode for lithium ion battery, RSC Adv. 5 (2015) 40737–40741.
[50] C. Tian, G. Wang, Study on the anti-tumor effect of polysaccharides from sweet potato, J. Biotechnol. 136 (2008) S351.
[51] Z. Zhang, J. Hao, J. Zhang, B. Zhang, J. Tang, Protein as the source for synthesizing fluorescent carbon dots by a one-pot hydrothermal route, RSC Adv. 2 (2012) 8599–8601.
[52] Q. Wang, X. Huang, Y. Long, X. Wang, H. Zhang, R. Zhu, L. Liang, P. Teng, H. Zheng, Hollow luminescent carbon dots for drug delivery, Carbon 59 (2013) 192–199.
[53] V.N. Mehta, S. Jha, S.K. Kailasa, One-pot green synthesis of carbon dots by using *Saccharum officinarum* juice for fluorescent imaging of bacteria (*Escherichia coli*) and yeast (*Saccharomyces cerevisiae*) cells, Mater. Sci. Eng. C 38 (2014) 20–27.
[54] A. Barati, M. Shamsipur, E. Arkan, L. Hosseinzadeh, H. Abdollahi, Synthesis of biocompatible and highly photoluminescent nitrogen doped carbon dots from lime: analytical applications and optimization using response surface methodology, Mater. Sci. Eng. C 47 (2015) 325–332.
[55] P. Roy, P.C. Chen, A.P. Periasamy, Y.N. Chen, H.T. Chang, Photoluminescent carbon nanodots: synthesis, physicochemical properties and analytical applications, Mater. Today 18 (2015) 447–458.
[56] A.M. Schwenke, S. Hoeppener, U.S. Schubert, Synthesis and modification of carbon nanomaterials utilizing microwave heating, Adv. Mater. 27 (2015) 4113–4141.
[57] X.M. Sun, Y.D. Li, Colloidal carbon spheres and their core/shell structures with noble-metal nanoparticles, Angew. Chem. Int. Ed. 43 (2004) 597–601.
[58] V.K. LaMer, Nucleation in phase transitions, Ind. Eng. Chem. 44 (1952) 1270–1278.
[59] S. Zhu, J. Zhang, S. Tang, C. Qiao, L. Wang, H. Wang, X. Liu, B. Li, Y. Li, W. Yu, Surface chemistry routes to modulate the photoluminescence of graphene quantum dots: from fluorescence mechanism to up-conversion bioimaging applications, Adv. Funct. Mater. 22 (2012) 4732–4740.
[60] Y.M. Long, C.H. Zhou, Z.L. Zhang, Z.Q. Tian, L. Bao, Y. Lin, D.W. Pang, Shifting and non-shifting fluorescence emitted by carbon nanodots, J. Mater. Chem. 22 (2012) 5917–5920.
[61] P. Dubey, K. Tripathi, M.R. Mishra, A. Bhati, A. Singh, S.K. Sonkar, A simple one-step hydrothermal route towards water solubilization of carbon quantum dots from soya-nuggets for imaging applications, RSC Adv. 5 (2015) 87528–87534.
[62] W. Lu, X. Qin, A.M. Asiri, A.O. Al-Youbi, X. Sun, Green synthesis of carbon nanodots as an effective fluorescent probe for sensitive and selective detection of mercury(II) ions, J. Nanopart. Res. 15 (2013) 1344–1351.
[63] C. Yu, T. Xuan, Y. Chen, Z. Zhao, Z. Sun, H. Li, A facile, green synthesis of highly fluorescent carbon nanoparticles from oatmeal for cell imaging, J. Mater. Chem. C 3 (2015) 9514–9518.
[64] S. Zhao, M. Lan, X. Zhu, H. Xue, T.W. Ng, X. Meng, C.S. Lee, P. Wang, W. Zhang, Green synthesis of bifunctional fluorescent carbon dots from garlic for cellular imaging and free radical scavenging, ACS Appl. Mater. Interfaces 7 (2015) 17054–17060.
[65] L. Wang, Y.D. Bi, J. Hou, H.Y. Li, Y. Xu, B. Wang, H. Ding, L. Ding, Facile, green and clean one-step synthesis of carbon dots from wool: application as a sensor for glyphosate detection based on the inner filter effect, Talanta 160 (2016) 268–275.
[66] Y.-W. Zeng, D.-K. Ma, W. Wang, J.-J. Chen, L. Zhou, Y.-Z. Zheng, K. Yu, S.-M. Huang, N, S co-doped carbon dots with orange luminescence synthesized through polymerization and carbonization reaction of amino acids, Appl. Surf. Sci. 342 (2015) 136–143.
[67] A. Isakovic, Z. Markovic, N. Nikolic, B. Todorovic-Markovic, S. Vranjes-Djuric, L. Harhaji, Inactivation of nanocrystalline C60 cytotoxicity by gamma - irradiation, Biomaterials 27 (2006) 5049–5058.